Ingeniería
Investigación y
Tecnología

Ambient seismic noise tomography to build up a 3D shear-wave velocity model

Tomografía sísmica de ruido ambiental para construir un modelo 3D de velocidad de onda de corte

Cárdenas-Soto Martín
Universidad Nacional Autónoma de México
Facultad de Ingeniería
E-mail: martinc@unam.mx
https://orcid.org/0000-0002-6586-469X

Piña-Flores José
Universidad Nacional Autónoma de México
Posgrado de Ingeniería
E-mail: jpf@unam.mx
https://orcid.org/0000-0002-4046-0322

Escobedo-Zenil David
Universidad Nacional Autónoma de México
Facultad de Ingeniería
E-mail: dezenil@unam.mx
https://orcid.org/0000-0001-8843-752X

Sánchez-González Jesús
Universidad Nacional Autónoma de México
Facultad de Ingeniería
E-mail: jsanchez@unam.mx
https://orcid.org/0000-0003-0471-3801

Martínez-González José Antonio
Universidad Nacional Autónoma de México
Facultad de Ingeniería
E-mail: josamago@gmail.com
https://orcid.org/0000-0001-7357-6308

Abstract

To explore the usefulness of the ambient seismic noise tomography method for characterizing the subsoil surface structure, in this study, we apply this method to contribute to geotechnical decision-making in the construction of a school building. We used a rectangular array (36 x 56 m) of 48-4.5 Hz vertical geophones and produce surface wave tomographies from the travel times of Rayleigh waves extracted by cross-correlation of seismic noise. We determined a final 3D Vs model using 1D models derived from the inversion of dispersion curves obtained from the tomography maps for different frequencies. The 3D model shows an excellent resolution (vertical and lateral); we observe critical velocity contrasts in the range of 2 to 15 m deep. At depths higher than 15 m, the velocity has values close to 900 m/s; however, we observe a low-velocity anomaly associated with a lava tube or crack that seems to continue under an adjacent building.

Keywords: Seismic interferometry, surface waves, site characterization, HVSR, lava tubes.

Resumen

A fin de explorar la utilidad del método de tomografía de interferometría de ruido sísmico ambiental para la caracterización de la estructura superficial del subsuelo, en este estudio aplicamos dicho método para contribuir a la toma de decisiones geotécnicas en la construcción de un edificio escolar. Para ello, utilizamos un arreglo rectangular (36 x 56 m) de 48 geófonos verticales con una respuesta en frecuencia de 4.5 Hz. A partir de la correlación cruzada del ruido sísmico, obtenemos tomografías de tiempo de viaje de la propagación de ondas superficiales tipo Rayleigh. Construimos un modelo final 3D de Vs utilizando modelos 1D generados de la inversión de las curvas de dispersión extraídas de los resultados de tomografía en diferentes frecuencias. El modelo 3D muestra una excelente resolución (vertical y lateral), lo cual nos permite identificar contrastes críticos de velocidad entre 2 y 15 m de profundidad. En profundidades mayores de 15 m, Vs tiene valores cercanos a 900 m/s, sin embargo, observamos una anomalía de baja velocidad asociada a un tubo de lava o fractura que parece continuar bajo el edificio adyacente.

Descriptores: Interferometría sísmica, ondas superficiales, caracterización de sitio, HVSR, tubos de lava.

Introduction

Ambient seismic noise has been widely used to study the seismic response of soft soil deposits using the horizontal-to-vertical spectral ratio (HVSR) (Nakamura, 1989; Field *et al.,* 1990; Bard, 1999). The main application of HVSR is seismic microzoning for cities mainly located in sedimentary basins (Lermo & Chávez, 1994ab; Field & Jacob, 1995). The seismic noise nature could be classified as that produced by natural activities at frequencies less than 1 Hz (Oceanic, Meteorological) and frequencies higher than 1 Hz produced by human activities (Bonnefoy *et al.,* 2006). In a broad frequency band, seismic noise is mainly formed by surface waves (e.g., Schuster, 2014). The extraction of the dispersive properties of these waves then allows determining the structure of S wave velocity of subsoil. The use of seismic noise has advantages over seismic methods using active sources. For example, studies are appropriated out in urban environments, and greater depth of penetration can be achieved through low-frequency seismic noise.

The use of station arrays has allowed the noise to be composed predominantly of surface waves. There are different microtremor analysis methodologies (Socco *et al.,* 2010) that seek to reliably determine the phase velocity dispersion curve of the fundamental mode of Rayleigh waves. The emphasis is on the characterization of the structure of the subsoil to have recognition advantages beyond what geotechnical techniques can provide (Okada, 2006). The most widely used and developed method, with regular and irregular arrays, is the spatial autocorrelation SPAC method (Wathelet *et al.,* 2008) proposed by Aki (1957). The method assumes that the seismic noise field is a stochastic stationary process in time and space. Under this assumption, Chávez *et al.* (2005) show that the dispersion characteristics of the surface waves contained in the noise can be extracted, operating only a couple of stations. In linear arrays, and similar to the active MASW method (Park *et al.,* 1999), the microtremor refraction method, ReMi (Louie 2001), offers a practical alternative to exploring the subsoil in the first tens of meters.

Among seismic noise methods, one method that can create a 3D representation of the structure of the subsoil (without the need for a source for mechanical wave generation) is ambient seismic noise interferometry tomography (ANT). Seismic interferometry (SI) makes use of cross-correlation of noise between pair stations to extract the so-called impulse response or Empirical Green Function (EGF) (e.g., Campillo & Paul, 2003; Draganov *et al.,* 2007; Schuster, 2014). The EGF is primarily formed by surface waves whose dispersion characteristics can be measured over a broad range of frequencies (Shapiro, 2004; Gouedard *et al.,* 2008). A summary of the historical background and a variety of applications in various fields of science can be found within, e.g., Schuster (2014), Larose *et al.* (2015).

In this study, we applied the ANT method to characterize the subsoil velocity structure at a site where a school building was currently built. The problem of the site is there are cavities or lava tubes due to basaltic spills from the eruption of the Xitle volcano, whose lava formed the so-called zone of the pedregal. Our objective is to explore subsoil discontinuities that can constitute a risk for building foundation. Because the method assumes the noise field contains surface waves that propagate in a stratified medium, in a first step, we explored the presence of a soft soil deposit employing the HVSR method in 16 measurements of ambient noise. Subsequently, we developed seismic noise tomography images from cross-correlations of the ambient noise recorded in a rectangular array with 48 vertical geophones. Ultimately, we present a 3D model of the shear wave velocity that we derive from the inversion of dispersion curves constructed from tomography images.

Study zone

The study site is located in the so-called Engineering Annex, which consists of a set of buildings of the School of Engineering at National Autonomous University of Mexico (UNAM). These buildings are constructed on a mixed base of soil and basalt rock characteristic of the university campus. The site is classified as a firm zone according to the geotechnical zoning of Mexico City (Lermo & Chávez, 1994a). In the area, the basaltic flows of the Xitle volcano stand out, whose eruption begins in a strombolian manner with a moderately explosive eruptive style (Siebe, 2009; Cervantes & Wallace, 2003). The successive eruptive stages resulted in lava flows that interspersed and overlapped with each other. These lavas descended at distances of approximately 12 km until reaching the southern plains of the valley of Mexico, where they covered the areas that currently occupy the urban developments of Tlalpan, Coyoacán, and Álvaro Obregón municipalities (Siebe, 2009). Because of the low viscosity and elevated temperature of the lava (>1000° C), these were solidified, leaving cavities or tunnels that are still preserved, as an example, the old name of Tlalpan, which in the nineteenth century was known as San Agustin de las Cuevas.

Figure 1 shows the location of the study site, which is limited by the parking areas of the faculty of accounting and administration (western side) and engineering

annex (eastern side). A road circuit is located to the south, and to the north, the building J, whose basement is irregularly shaped because it was adapted to the pre-existing morphology. At the site, we performed 16 measurements of ambient noise using Guralp system 6TD broadband triaxial seismographs. Next, we installed an array of 48 vertical geophones of 4.5 Hz with separations of 3 and 4 m to surround an approximate area of 36 x 56 m^2. The ambient seismic noise for tomography imaging was recorded for 60 min using four EX12 seismographs of Seistronix Instrument.

The horizontal-to-vertical spectral ratio (HVSR)

The HVSR, or commonly referred to as the Nakamura method (Nakamura, 1989), is used to evaluate the site effect, i.e., the relative amplification of the subsoil due to the presence of a soft soil layer and the frequency at which this amplification occurs. The method makes use of ambient seismic noise by assuming the wave field is predominantly formed by surface waves (Bonnefoy *et al.*, 2006). If the layer is present, the spectral ratio of the average Fourier amplitude spectra of horizontal components, among the amplitude spectrum of vertical component, provides the seismic response of the soft layer. The frequency where the maximum response appears is called the fundamental frequency of vibration of the soil layer (f_0). The Nakamura method represents a suitable approach to amplification due to S-wave resonance (Lermo & Chávez, 1994b). Therefore, it is possible to approximate the thickness of the soft soil layer (if it exists) by the formulation $f_0 = \beta / 4H$.
Where:

f_0 = fundamental frequency
β = shear-wave velocity and
H = layer thickness

In the assessment of the HVSR, we used 30 min of ambient noise recording to obtain the average spectral ratio result of windows of 40s duration with an overlap of 50 %. In this estimate, the spectra were smoothed by a Konno-Ohmachi window (Konno & Ohmachi, 1998) with a smoothening fraction of 20 %.

Figure 2 shows the average HVSR curves of the 16 measurement points shown in Figure 1. Except for points P and L, the results show well-defined spectral ratios with an average relative amplification between 2 and 3. These ratios convincingly indicate the distribution of unconsolidated materials overlaying a more competent layer (interpretation criterion according to the SESAME guidelines; Bard and SESAME-Team, 2004). The range of

vibrating frequencies that define these ratios is 4.5 to 7.0 Hz, indicating the variability of the thickness of the unconsolidated materials or the irregularity of the sublayer. If we consider that the average fundamental frequency of the 16 measuring points is 5.4 Hz and an average Vs velocity of 350 m/s (which we will demonstrate later), then the substratum depth is about 16 m. Some of the stations (F, G, H, J, and P) show a second peak near the frequency of 20 Hz with amplitude almost similar to the first peak. We can attribute that this second peak is related to an impedance contrast caused by a surface layer, which can behave independently of the entire soil column (Guéguen *et al.*, 1998; Macau *et al.*, 2015). The presence of unconsolidated materials in the study area seems extraordinary because we have described an area of basaltic materials. However, site recognition shows volumes of highly fractured volcanic material with an irregular distribution of filling areas, as is showed in the image of Figure 1.

Ambient noise tomography

Noise records are usually preprocessed to retain the stationary part of the background noise (Bensen *et al.*, 2007). In this process, an equalization of the Fourier spectrum (spectral whitening) of the noise recorded is performed so that there are contributions of the energy associated with the distinct phases. From the normalized records, we carry out cross-correlations between all pairs of receivers. In this work, we have chosen to cross-correlate windows of 60 s of overlapping duration 50 % over the 60 min of time record. In Figure 3a, we show the virtual source section 01, the result of the cross-correlation of the noise record of the receiver 01 with the remaining records of the 48 receivers. In this figure, it is observed that wave trains emerge whose amplitude is remarkable in time delays less than 1 s. The pulses have a high signal to noise ratio and emerge consistently either in the anti-causal part (times less than zero) or causal (times greater than zero). The correlation pulses between the receivers 01 and 10 show a sudden change in velocity from receiver 06. Between receivers, 10 and 19 phases and amplitude are lost in some receiver. In Figure 3b, we show the virtual source section of the receiver 25. Variations in the correlation pulse and the presence of secondary wave trains are observed in receivers 01 to 08 and 41 to 48. Moreover, at short distances (receivers 30 to 33), the correlation pulse loses its shape. Results similar to those shown in Figure 3 can be observed for the other 48 virtual source sections.

The symmetry of the pulses in the cross-correlation function is related to the equipartition condition,
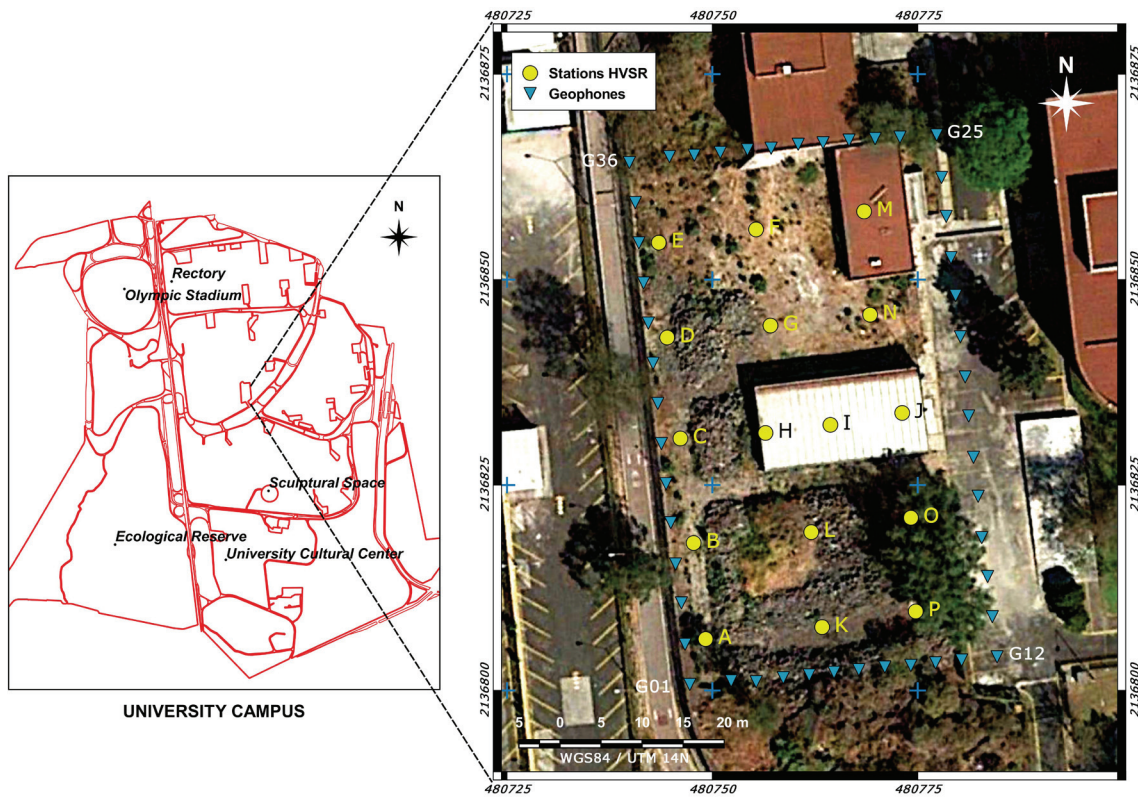
Figure 1. Study site. The blue triangles show the position of the 4.5 Hz vertical geophones. The vertices of the array are indicated with the nomenclature denoting the geophone number G01, G12, G25, and G36. The yellow circles denoted by the letters A to P indicate the points where the HVSR was applied
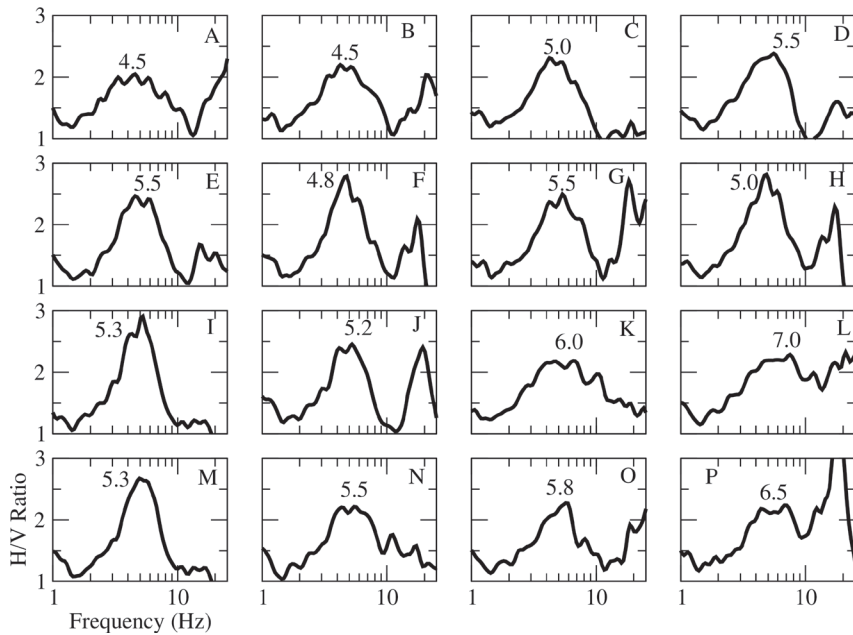

Figure 2. Mean HVSR curves of each of the recording points within the study area (Figure 1). The number within each graph indicates the maximum frequency of the HVSR, which can be interpreted as the proper frequency of vibration of the soil layer. In the upper right corner of each graph is indicated the letter denoting each measurement point
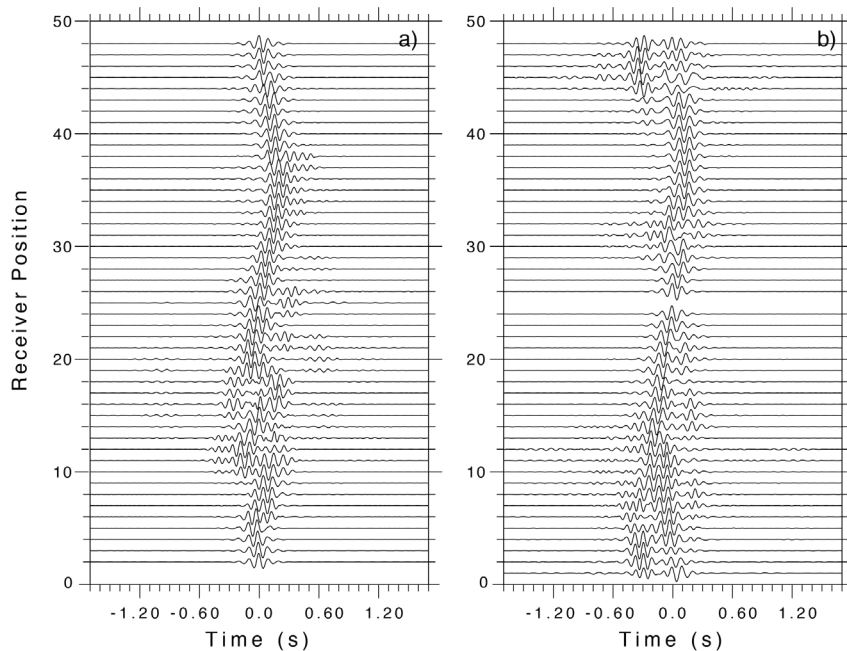
Figure 3. Virtual source sections result from the correlation of the record in receiver: a) 01 and b) 25, concerning the remaining 48. Traces are filtered between 5 and 15 Hz

which must be completely satisfied to obtain the EGF. This condition is fundamental in IS under the view that the wavefield in a closed system should consist of arbitrary contributions of all possible modes of propagation, with equal weight on average (Weaver & Lobkis, 1982; Schuster, 2014). If the medium contains a sufficient distribution of scatters, then it is possible to satisfy the condition of equipartition with an unique source because each scatter acts as a secondary source. In open systems, the most appropriate definition of equipartition states that the flow of energy must be equal in all directions (e.g., Snieder *et al.*, 2007). For practical purposes, the emergence of EGF either in the causal or anti-causal part can be used to characterize the subsoil, as it is enough to add the anti-causal part to the causal part to increase the coherence of the pulse. The extraction of the correlation pulse or EGF) is because the primary source of seismic noise is due to vehicular traffic (Halliday *et al.*, 2011) that occurs in the road circuit near the study area.

The emphasis of this study is to characterize the lateral variations of subsoil velocity. For this, we exploited the position of the delay times of the envelope maximum of the correlograms filtered in different frequencies (Cárdenas *et al.*, 2016). The identification of travel time (maximum correlation pulse) at different frequencies can then be used to produce a tomography image that provides the distribution of the velocity of the medium separating two receivers (Shapiro *et al.*, 2005; Sabra *et al.*, 2005).

We used the filtered virtual source sections and extracted the maximum delay times from the envelope of the correlation pulse for 36 central frequencies generated from a mobile filter whose width is a function of the frequency for the range of 4 to 24 Hz. From those times, we built travel time tomographies to know the distribution of the group velocity. The study area was discretized by a mesh whose cells were 4 m per side, where the number of pairs of trajectories (rays) that covered the mesh, for 48 receivers (n=48), was n(n–1)/2=1128. The inversion processes were carried out by Simultaneous Interaction Reconstruction Tomographic (SIRT) method (Nolet & Wapenaar, 2009) to derive phase velocity distributions. The inversion process was further improved by incorporating the maximum slope method (Arfken *et al.*, 1999), which minimizes the objective function. The objective function is defined as the difference between the observed data and the synthetic calculated data produced by the forward modeling, and sometimes with another term of regularization or damping (Uieda *et al.*, 2013).

Figure 4 shows as an example, the images of the results at the frequencies of 6, 8, and 12 Hz. The color scale is different for each image to highlight the contrasts between the resolved phase velocity values. This contrast results between the mean phase velocity of 250 m/s and 500 m/s. The existence of velocity values of 250 m/s at low frequencies, such as 6 Hz, indicates that in-depth little consolidated materials prevail in the East and West of the study site. At 6 Hz, velocity values hig-

her than 650 m/s are observed concerning the results of the images at 8 and 12 Hz. High-velocity values at low frequencies indicate the presence of more compact material in depth. A high-speed anomaly highlights at the center of the array on all three frequencies. The distribution of high velocities to the south, center, and northwest part of the array is consistent with the distribution of basaltic materials observed at the site. In general, the resolved velocity at low frequencies is higher than at intermediate and high frequencies. This behavior is characteristic of the dispersion property of surface waves, the variation of velocity as a function of frequency.

The frequency-dependent velocity variation at each node of the tomography model is shown in Figure 5a. These values describe phase velocity dispersion curves of Rayleigh waves. The curves show that at frequencies close to 4 Hz (limit of the characteristic frequency of geophones), the phase velocities can be between 400 and 1400 m/s. Most curves describe velocity values between 400 and 600 m/s. for frequencies higher than 6 Hz, the decay of the curves shows values between 200 and 500 m/s. The curves shape in Figure 5a indicates they can reasonably be inverted to obtain a shear wave velocity profile. Figure 5b shows an example of the inversion of a dispersion curve (Herrmann, 2013). The procedure consisted of proposing a model of 11 layers whose thickness increases with the depth at a constant velocity (in this case, 600 m/s). After several interactions, the inversion method converges to provide a Vs velocity profile. The example in Figure 5b shows excellent convergence towards the final model.

We have constructed a volume of shear wave velocity as a function of depth (Voxler 4.0 Software) from the 1D profiles resulting from the inversion of each of the dispersion curves. Figure 6 shows the 3D model of this volume, where we have highlighted two isosurfaces that describe in a general way the subsoil structure in the study area. The first of them has a value of 700 m/s and indicates the limit of poorly consolidated materials distributed heterogeneously between the surface and approximately 16 m deep. As discussed in the section on HVSR spectral ratios (Figure 2), this depth is consistent with that suggested by the 1D model of short-wave propagation (Equation 1). The depth at which the substratum is located was also determined by Sanchez (2019) from join inversion results of the HVSR and dispersion curves obtained by SPAC (Aki, 1957) and f-k (Capon, 1969) methods.

The second isosurface corresponds to the lowest velocity values (close to 300 m/s). The distribution of these values should be located close to the surface of the terrain. However, a low-velocity anomaly is observed between 10 and 20 m deep, which extends inward of the array to a distance of approximately 30 m. The anomaly coincides with an old crack located below the adjacent building. Most likely, that crack or lava tube is filled with tuffs and fractured materials. We observe that the low-velocity anomaly emerges due to inconsistent time delays of the correlation pulses. The irregularity of the correlation pulses described above suggests it is a cavity-like structure that probably causes resonance in the wave field extracted by SI (Catheline *et al.*, 2008; Hillers *et al.*, 2014, Argote *et al.*, 2020).
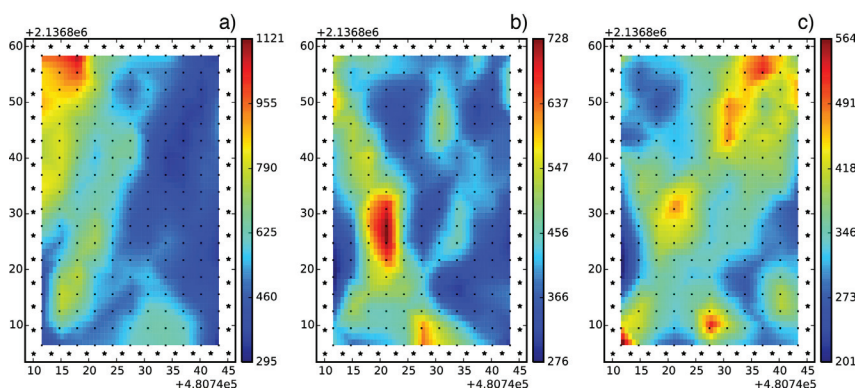

Figure 4. Seismic noise tomography at frequencies of 6, 8 and 12 Hz, a), b) and c) respectively. The phase velocity distribution (m/s) in a UTM reference system is displayed. The black stars indicate the position of the geophones. The black dots represent the Centers of the cells where the tomography method is solved. The color scale indicates the phase velocity values, and it is different for each image
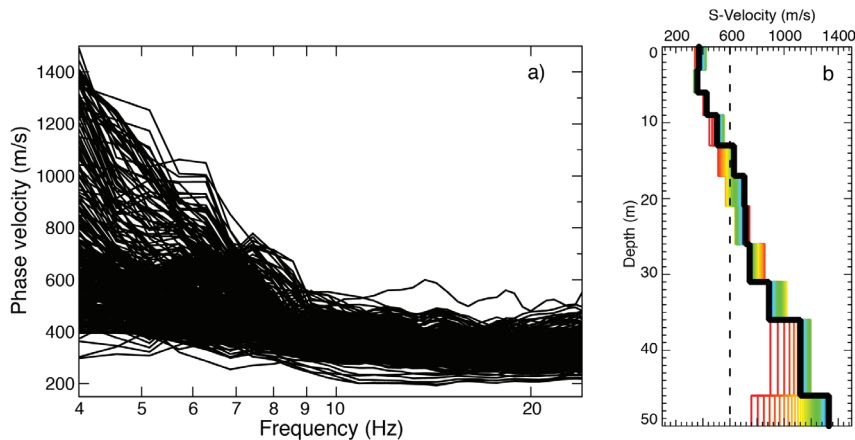
Figure 5. a) Dispersion curves obtained from travel time tomography, b) shear wave velocity profile resulting from the inversion of a dispersion curve. The discontinuous black line is the initial velocity model. The colored lines represent the different solved models until they converge to the final model (black line)
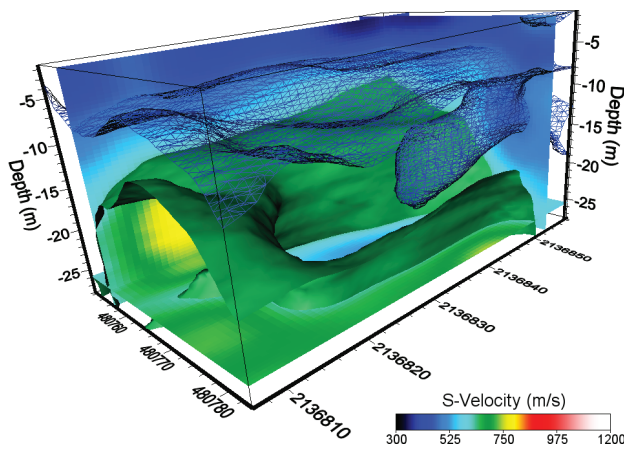

Figure 6. Shear wave velocity model produced by the interpolation of 1D Vs profiles obtained from the tomographic results. Two isosurfaces are shown; at 700 m/s (green) and 300 m/s (blue lines)

Conclusions

The use of ambient seismic noise to characterize subsurface structure is widely used, but its applicability must consider some limitations. For example, the HVSR method works if there are significant contrasts of mechanical properties in-depth. The SI method requires an adequate azimuthal distribution of noise sources to recover the medium response adequately. These two requirements were found in the site study. HVSR spectral ratios showed a clear site response, and it was possible to extract correlation pulses due to secondary noise sources produced by the volcanic materials.

The 3D-Vs model obtained exhibits lateral and vertical variations of shear wave velocity and an irregular substratum. Although the site is geotechnically classified as firm soil, HVSR results indicate the existence of a layered structure whose surface materials produce relative amplification in the frequency range of 4.5 to 7.0 Hz. Such materials correspond to altered basalts combined with filler materials. According to HVSR peak frequencies, soft soil deposits have an average thickness of 12 m.

The cross-correlation functions extracted by SI indicate the seismic noise propagates precisely in a layered structure. In some trajectories, there are delayed or incoherent correlation pulses that define low-velocity zones. These functions correspond to Rayleigh surface waves whose dispersion characteristics allowed us to produce seismic tomography images of phase velocity in the range of 4 to 24 Hz. The 3D model built from the dispersion curves obtained from ANT shows an average velocity of 300 m/s for surface materials and 800 m/s for depths higher than 12 m. A low-velocity anomaly is also observed near the adjacent building, which correlates with an old preexistent crack or lava tube filled during the building construction.

This study shows that ambient seismic noise tomography can help define a subsoil structure model with lateral velocity variations. The model is valuable for tracking the seismic response of the site. We believe in future studies; it will also allow us to know changes in

subsoil behavior to prevent damages in the building that is now is erected.

This methodology can be applied to other sites with different geological conditions. Future work includes incorporating joint inversion methods between dispersion curves and HVSR spectral ratios and improving the seismic tomography scheme for smaller arrays. It is also necessary to integrate geophysical methods like electrical tomography and gravimetry and confront the results with geotechnical studies.

REFERENCES

Aki, K. (1957). Space and time spectra of stationary stochastic waves, with special reference to microtremors, Tokyo University. *Bulletin of the Earthquake Research Institute*, 25, 415-457 http://eprints.uni-kiel.de/id/eprint/43280

Argote, D. L., Tejero, A., Cárdenas, M., Cifuentes, G., Chávez, R. E., Hernández & Ortega, V. (2020). Designing the underworld in Teotihuacan: Cave detection beneath the moon pyramid by ERT and ANT surveys. *Journal of Archaeological Science*, 118, 105141.

Arfken, G. B., Weber, H. J. & Spector, D. (1999). Mathematical methods for physicists, 4th ed. *American Journal of Physicists*, 67(2), 165-169.

Bard, P-Y. (1999). Microtremor measurements: a tool for site effect estimation? In: Irikura K., Kudo K., Okada H., Sasatani T. (eds) The effects of surface geology on seismic motion, Balkema, Rotterdam, 1251-1279

Bard, PY SESAME-Team. (2004). Guidelines for the implementation of the H/V spectral ratio technique on ambient vibrations-measurements, processing and interpretations, SESAME European research project EVG1-CT-2000-00026, deliverable D23.12. http://www.sesame-fp5.obs.ujf-grenoble.fr Accessed March 2020

Bensen, G. D., Ritzwoller, M. H., Barmin, M. P., Levshin, A. L., Lin, F., Moschetti, M. P., Shapiro, N. M., & Yang, Y. (2007). Processing seismic ambient noise data to obtain reliable broad-band surface wave dispersion measurements. *Geophysical Journal International*, 169(3), 1239-1260. https://doiorg/10.1111/j.1365-246X.2007.03374.x

Bonnefoy, S., Cotton, F. & Bard, P. Y. (2006). The nature of noise wavefield and its applications for site effects studies: A literature review. *Earth-Science Reviews*, 79(3-4), 205-227. https://doi.org/10.1016/j.earscirev.2006.07.004

Campillo, M. & Paul, A. (2003). Long range correlations in the diffuse seismic coda. *Science*, 299, 547-549. https://doi.org/10.1126/science.1078551

Capon, J. (1969). High-resolution frequency-wavenumber spectrum analysis. *Proceedings of the IEEE*, 57(8), 1408-1418. https://doi.org/10.1109/PROC.1969.7278

Cárdenas, M., Ramos, H. & Vidal, M. C. (2016). Interferometría de ruido sísmico para la caracterización de la estructura de velocidad 3D de un talud en la 3a Sección del Bosque de Chapultepec, Ciudad de México. *Boletín de la Sociedad Geológica Mexicana* (in Spanish), 68(2), 173-186.

Catheline, S., Benech, N., Brum, J. & Negreira, C. (2008). Time reversal of elastic waves in soft solids. *Physical Review Letters*, 100(6), 064301. https://doi.org/10.1103/PhysRevLett.100.064301

Cervantes, P. & Wallace, P. (2003). Magma degassing and basaltic eruption styles: a case study of ~2000 year BP Xitle volcano in central Mexico. *Journal of Volcanology and Geothermal Research*, 120, 249-270. https://doi.org/10.1016/S0377-0273(02)00401-8

Chavez, F. J., Rodriguez, M. & Stephenson, W.R. (2005). An alternative approach to the SPAC analysis of microtremors: exploiting stationarity of noise. *Bulletin Seismological of Society America*, 95(1), 277-293. https://doi.org/10.1785/0120030179

Draganov, D. S., Wapenaar, K., Mulder, W., Singer, J. & Verdel, A. (2007). Retrieval of reflections from seismic background-noise measurements. *Geophysics Research Letters*, 34(4), 2-5.

Guéguen, P., Chatelain J. L., Guillier B., Yepes, H. & Egred, J. (1998), Site effect and damage distribution in Pujili (Ecuador) after the 28 March 1996 earthquake. *Soil Dynamics and Earthquake Engineering*, 17, 329-334.

Gouedard, P., Stehly, L., Brenguier, F., Campillo, M., De Verdière, Y. C., Larose, E. & Weaver, R. L. (2008). Cross-correlation of random fields: Mathematical approach and applications. *Geophysical prospecting*, 56(3), 375-393. https://doi.org/10.1111/j.1365-2478.2007.00684.x

Halliday, D. (2011). Adaptive interferometry for ground-roll suppression. *The Leading Edge*, 30(5), 532-537. https://doi.org/10.1190/1.3589110

Helffrich G., Wookey J. & Bastow I. (2013). *The seismic analysis code: A primer and user's guide*. 1st ed. United Kingdom: Cambridge University Press.

Herrmann R. B. (2013). Computer programs in seismology: An evolving tool for instruction and research. *Seismological Research Letter*, 84(6), 1081-1088. https://doi.org/10.1785/0220110096

Hillers, G., Campillo, M., Ben-Zion, Y. & Roux, P. (2014). Seismic fault zone trapped noise. *Journal Geophysical Research, Solid Earth*, 119(7), 5786-5799. https://doi.org/10.1002/2014JB011217

Konno, K. & Ohmachi, T. (1998). Ground-motion characteristics estimated from spectral ratio between horizontal and vertical components of microtremor. *Bulletin of the Seismological Society of America*, 88(1), 228-241.

Larose, E., Carrière, S., Voisin, C., Bottelin, P., Baillet, L., Guéguen, P. & Gimbert, F. (2015). Environmental seismology: What can we learn on earth surface processes with ambient noise. *Journal of Applied Geophysics*, 116, 62-74. https://doi.org/10.1016/j.jappgeo.2015.02.001

Lermo, J. & Chávez, F. J. (1994a). Site effect evaluation at Mexico City: dominant period and relative amplification from strong motion and microtremor records. *Soil Dynamics and Earthquake Engineering*, 13(6), 413-423.

Lermo, J. & Chávez, F. J. (1994b). Are microtremors useful in site response evaluation? *Bulletin of the Seismological Society of America*, 84, 1350-1364.

Louie, J. N. (2001). Faster, better: shear-wave velocity to 100 meters depth from refraction microtremor arrays. *Bulletin of the Seismological Society of America*, 91, 347-364. https://doi.org/10.1785/0120000098

Field, E. H., Hough, S.E. & Jacob, K. H. (1990), Using microtremors to asses potential earthquake site response: a case study in Flushing Meadows, New York City. *Bulletin of the Seismological Society of America*, 80, 1456-1480.

Field, E. H. & Jacob, K. H. (1995). A comparison and test of various site response estimation techniques, including three that are not reference site dependent. *Bulletin of the Seismological Society of America*, 85, 1127-1143.

Macau, A., Benjumea, B., Gabàs, A., Figueras, S. & Vilà, M. (2015). The effect of shallow quaternary deposits on the shape of the H/V spectral ratio. *Surveys in Geophysics*, 36(1), 185-208.

Nakamura, Y. (1989). A method for dynamic characteristics estimation of subsurface using microtremor on the ground surface. *Q. Rep. Railway Tech. Res. Inst.*, 30(1), 25-33.

Nolet G. & Wapenaar K. (2009). A breviary of seismic tomography: Imaging the interior of the Earth and the Sun. *Journal of the Acoustical Society of America*, 126(4), 2129.

Park, C. B., Miller, R. D. & and Xia, J. (1999). Multichannel analysis of surface waves. *Geophysics*, 64(3), 800-808.

Okada, H. (2006). Theory of efficient array observations of microtremors with special reference to the SPAC method. *Exploration Geophysics*, 37(1), 73-85.

Sabra, K. G., Gerstoft, P., Roux, P., Kuperman, W. A. & Fehler, M. C. (2005). Extracting time-domain Green's function estimates from ambient seismic noise. *Geophysical Research Letters*, 32(3). https://ui.adsabs.harvard.edu/link_gateway/2005GeoRL..32.3310S/doi:10.1029/2004GL021862

Sánchez, R. (2019). *Técnicas de ruido sísmico para la obtención de un modelo 3D de velocidad de onda S en el Anexo de Ingeniería, Ciudad Universitaria* (B.S. Thesis), Facultad de Ingeniería, UNAM (in Spanish). http://132.248.9.195/ptd2019/octubre/0797059/Idex.html

Schuster, G. T. (2014). *Seismic interferometry*. Encyclopedia of Exploration Geophysics, Q1-1-, Q1-41.

Shapiro, N. M. (2004). Emergence of broadband Rayleigh waves from correlations of the ambient seismic noise. Geophysical Research Letters, 31, L07614. https://doi.org/10.1029/2004GL019491

Shapiro, N. M., Campillo, M., Stehly, L. and Ritzwoller, M. H. (2005). High-resolution surface-wave tomography from ambient seismic noise. *Science*, 307(5715), 1615-1618. https://doi.org/10.1126/science.1108339

Siebe, C. (2009). *La erupción del volcán Xitle y las lavas del Pedregal hace 1670 +/-35 años AP y sus implicaciones*. Biodiversidad del ecosistema del Pedregal de San Ángel, Universidad Nacional Autónoma de México (in Spanish): Lot A, Cano-Santana Z. (eds), 43-50.

Snieder, R., Wapenaar, K. & Wegler, U. (2007). Unified Green's function retrieval by cross correlation: Connection with energy principles. *Physical Review E., Statistical, nonlinear, and soft matter physics*, 75(3), part 2, 036103. https://doi.org/10.1103/physreve.75.036103

Socco, L. V., Foti, S. & Boiero, D. (2010). Surface-wave analysis for building near-surface velocity models established approaches and new perspectives. *Geophysics*, 75(5), 75A83-75A102. https://doi.org/10.1190/1.3479491

Uieda L., Oliveira Jr V. C. & Barbosa V.C. (2013). Modeling the Earth with Fatiando a Terra. In: Proceedings of the 12th Python in Science Conference, 90-96. https://doi.org/10.25080/Majora-8b375195-010

Wathelet, M., Jongmans, D., Ohrnberger, M. & Bonnefoy-Claudet, S. (2008), Array performances for ambient vibrations on a shallow structure and consequences over Vs inversion. *Journal of Seismology*, 12(1), 1-19.

Weaver, R. & Lobkis, O. (2002). On the emergence of the Green's function in the correlations of a diffuse field: Pulse-echo using thermal phonons. *Ultrasonics*, 40(1-8), 435-439.